

LANGUAGE GUIDED DOMAIN GENERALIZED MEDICAL IMAGE SEGMENTATION

*Shahina Kunhimon*¹, *Muzammal Naseer*¹, *Salman Khan*¹, *Fahad Shahbaz Khan*^{1,2}

¹ Mohamed bin Zayed University of Artificial Intelligence - UAE,

² Linkoping University - Sweden

ABSTRACT

Single source domain generalization (SDG) holds promise for more reliable and consistent image segmentation across real-world clinical settings particularly in the medical domain, where data privacy and acquisition cost constraints often limit the availability of diverse datasets. Depending solely on visual features hampers the model’s capacity to adapt effectively to various domains, primarily because of the presence of spurious correlations and domain-specific characteristics embedded within the image features. Incorporating text features alongside visual features is a potential solution to enhance the model’s understanding of the data, as it goes beyond pixel-level information to provide valuable context. Textual cues describing the anatomical structures, their appearances, and variations across various imaging modalities can guide the model in domain adaptation, ultimately contributing to more robust and consistent segmentation. In this paper, we propose an approach that explicitly leverages textual information by incorporating a contrastive learning mechanism guided by the text encoder features to learn a more robust feature representation. We assess the effectiveness of our text-guided contrastive feature alignment technique in various scenarios, including cross-modality, cross-sequence, and cross-site settings for different segmentation tasks. Our approach achieves favorable performance against existing methods in literature. Our code and model weights are available at https://github.com/ShahinaKK/LG_SDG.git.

Index Terms— Multi-modal contrastive learning, Medical image segmentation, Single source domain generalization.

1. INTRODUCTION

The generalizability of deep learning-based medical segmentation models often gets compromised by the domain shift between training and test datasets. The discrepancies in the data acquisition process such as imaging modalities, equipment characteristics, and scanning protocols are the main contributing factors for this distribution shift which is considered as a primary hurdle in their clinical deployment [1]. Unsupervised Domain Adaptation (UDA) [2] and Multi-Source Domain Generalization (MSDG) [3] approaches, designed to mitigate acquisition shifts, pose practical challenges. These

methods depend on training data from the target or multiple source domains, which can be difficult to procure due to cost and privacy concerns. Single Source Domain Generalization (SDG) is a more practical setting for training networks that can handle unseen domains, using training data from a single source domain. Existing SDG techniques leverage techniques such as data augmentation [4, 5], feature adaptation [6, 7] to improve the data diversity and to enhance the model’s generalization capabilities. However, SDG comes with its own set of challenges. A segmentation model trained on a single source can overfit limiting its ability to generalize to unseen domains. The overfitting arises due to : (i) Dependence on source domain-specific features such as image intensity and texture. For example, in liver segmentation from CT images, liver appears as a high-intensity structure against dark background, creating strong contrast. On the other hand, in T2-SPIR MRI images, liver exhibits varying signal intensities due to water content differences within the structure. (ii) Spurious correlations due to the confounding variables present in the training image background. For instance, scans from different hospitals may contain varying background objects unrelated to the region of interest (ROI). However, the model might mistakenly correlate them with ROIs when trained on single source data hindering its performance.

To tackle these challenges associated with relying solely on visual features, we utilize language models to communicate visual cues about the ROIs across different domains [8]. During training on a single domain such as CT, we also provide clear descriptions regarding the ROI or label’s characteristics including its intensity and structural attributes across both source and target domains (CT and MRI). This multi-domain knowledge equips the model to generalize its understanding from source to target (CT to MRI) and vice versa [9, 10]. We introduce a contrastive approach that aligns textual features with image features, enabling the model to prioritize clinical context over misleading visual correlations. This facilitates the mapping of specific text features to corresponding visual patterns. Our contributions are as follows:

- We enhance state-of-the-art SDG methods for medical image segmentation by integrating a text-guided contrastive feature alignment module into the training pipeline. This provides a domain-agnostic perspective, reducing sensitivity to domain shifts and spurious correlations by

grounding visual features with textual information.

- Our proposed approach is complementary and can be seamlessly integrated into any segmentation network without architectural modifications.
- We evaluate our text-guided contrastive feature alignment method in various challenging scenarios including cross-modality, cross-sequence, and cross-site settings for the segmentation of diverse anatomical structures.

2. RELATED WORK

SDG methods strive to create robust segmentation models that perform consistently across various clinical scenarios, even in the face of domain shifts caused by differences in acquisition process. The existing SDG approaches can be mainly categorized into two: (i) Image level adaptation methods such as [4, 5, 11, 12] which utilizes data augmentation strategies to improve training data diversity and (ii) Image and feature level adaptation methods like [6, 7] which focuses on adapting the feature level representations as well. Recently, a causality-inspired data augmentation approach CSDG was introduced in [4] to mitigate the impact of spurious correlations through causal intervention. Another augmentation based contrastive SDA approach called SLAug was proposed in [5] which incorporated class-level information into the augmentation process in order to improve the generalization performance. Among the image and feature level adaptation models, a dual-normalization based method introduced in [6] followed a contrastive approach utilizing source-similar or source dissimilar training examples. It performed well under cross-modality settings but its performance is sub-optimal in the cross-site problem setting. CCSDG approach from [7] attempts to improve the generalization performance across data from various centres by utilizing a contrastive feature disentanglement step to filter out the style-sensitive channel representations to enhance the image feature representations.

3. METHOD

SDG provides a practical solution to mitigate performance degradation caused by distribution shifts in medical image segmentation models. Instead of requiring data from multiple sources or target domains, SDG focuses on training the network on single source dataset $\mathcal{D}^s = \{x, y\}$ where x represents the image and y corresponds to the ground truth, with the objective of generalizing well to unseen target domains.

Different from existing approaches, our approach addresses the SDG problem in medical image segmentation by exploiting well-structured language models that have already been trained on large-scale datasets. We use ChatGPT to generate diverse organ-specific text descriptions for all the possible segmentation classes. For instance; in the cross-modality (CT/MRI) experiments on Abdomen dataset, we

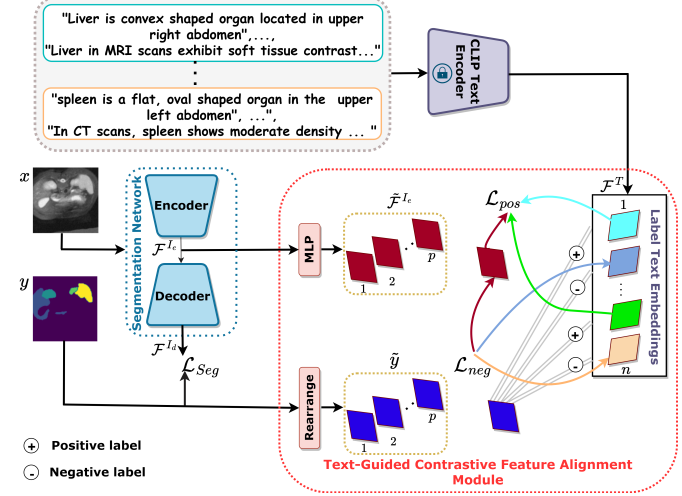


Fig. 1. The proposed training pipeline consists of (i) **Segmentation network**: an encoder-decoder model (ii) **CLIP Text Encoder**: which is frozen and takes text descriptions from ChatGPT as input to create label-wise text embeddings and (iii) **Text-Guided Contrastive Feature Alignment Module**: which enhances the alignment between the image and text encoder representations via our feature-level contrastive loss.

pass the following query to ChatGPT: *“Describe the appearance, texture, size, shape, intensity and other characteristics to distinguish the liver, right kidney, left kidney, and spleen from each other in CT and MRI”*. Sample Response: *“The liver in CT images appears as a high-intensity structure with uniform texture whereas in MRI, the liver exhibits varying signal intensities.”* These descriptions capture various facets of labels to distinguish them across source and target domains. It’s important to note that not all image crops necessarily contain all segmentation classes and there can be instances where anatomical structures overlap or share visual traits. To address these class-level ambiguities, we introduce a text-guided contrastive feature alignment (TGCFA) module. This module extracts class-level information from ground truth, to guide image representation learning so that the visual features learned lie closer to the text embeddings of the positive classes. The proposed method incorporates a text encoder and TGCFA module complementing the baseline image segmentation network as shown in Fig.1. **Baseline Segmentation Network:** We employ a U-shaped encoder-decoder network \mathcal{F}^I as the segmentation backbone. For each image x , the segmentation network outputs the encoded feature vector $\mathcal{F}^{I_e} \in \mathbb{R}^{p \times z}$ and segmentation prediction \mathcal{F}^{I_d} , where p denotes the number of features and z represents the embedding dimension of each feature. The final segmentation mask (\mathcal{F}^{I_d}) is compared with ground truth y to optimize the segmentation objective (\mathcal{L}_{Seg}) such as cross-entropy or dice loss. The encoder representation (\mathcal{F}^{I_e}) is then fed to our TGCFA module for text-guided contrastive feature alignment. **Text**

Table 1. Details of the Cross-Domain Segmentation datasets and the source-target splits used for evaluation

Name	Dataset	Labels	Split	Domains	No. of scans
Abdomen cross-modality	SABSCIT [13]	Liver, Right kidney, Left kidney, Spleen	Source/Target	CT	30
	CHAOS [14]		Target/Source	MRI	20
Cardiac cross-sequence	MS-CMR [15]	Myocardium, Left ventricle, Right ventricle	Source/Target	balanced steady-state free precession(bSSFP)	45
			Target/Source	late gadolinium enhanced(LGE)	45
Fundus cross-site	RIGA+ [16]	Optic Disc, Optic Cup	1 source 3 target	BinRushed/Magarabia BASE 1, BASE 2, BASE 3	195, 95 173, 148, 133

Table 2. For Cross-Modality Experiments (Left): Our approach consistently improves the organ-wise results and narrows down the gap between SDG and supervised upperbound (trained and tested in target domain). For Cross-Sequence Experiments (Right): Our approach improves the average dice score in both directions. The highest scores in SDG setting are highlighted.

Method	Cross Modality (Abdominal CT-MRI)					Cross-Sequence (Cardiac bSSFP-LGE)			
	Liver	Right Kidney	Left Kidney	Spleen	Average	Left Ventricle	Myocardium	Right Ventricle	Average
Supervised	91.30	92.43	89.86	89.83	90.85	92.04	83.11	89.30	88.15
	90.08	89.23	87.54	87.67	88.63	91.53	80.65	87.90	86.69
	90.52	89.54	88.21	88.44	89.18	91.50	81.10	88.24	86.95
Method	Cross Modality (Abdominal MRI-CT)					Cross-Sequence (Cardiac LGE-bSSFP)			
	Liver	Right Kidney	Left Kidney	Spleen	Average	Left Ventricle	Myocardium	Right Ventricle	Average
	98.87	92.11	91.75	88.55	92.82	91.16	82.93	90.39	88.16
	89.26	80.98	82.05	79.93	83.05	91.92	81.49	89.61	87.67
SLAug(Ours)	90.34	84.14	82.15	84.76	85.35	91.87	81.93	89.88	87.89

Encoder: We leverage a pretrained CLIP [17] text encoder which remains frozen to map the label descriptions to text feature representation. Specifically, for an n -class segmentation problem, we generate v variations of text descriptions for each of the n labels as $t_r = \{t_{r1}, t_{r2}, \dots, t_{rv}\}_{r=1}^n$. These descriptions are tokenized and passed through pretrained CLIP text encoder to get corresponding text embeddings $O_r = \{O_{r1}, O_{r2}, \dots, O_{rv}\}_{r=1}^n$. We compute the mean representation for each label to get the text feature vector $\mathcal{F}_r^T \in \mathbb{R}^k$ for label r where k is the dimensionality of text representation i.e, the final text feature representation is given by:

$$\mathcal{F}^T = \{\mathcal{F}_1^T, \mathcal{F}_2^T, \dots, \mathcal{F}_n^T\}$$

$$\text{where } \mathcal{F}_r^T = \frac{\Sigma(O_{r1}, O_{r2}, \dots, O_{rv})}{v} \in \mathbb{R}^k \quad (1)$$

Text-Guided Contrastive Feature Alignment (TGCFA) module: The text representations \mathcal{F}^T and image encoder output \mathcal{F}^{I_e} along with the ground truth y are used in the TGCFA module to learn the multi-modal feature alignment objective. To make the multi-modal (image and text) representations consistent, the visual encoder features $\mathcal{F}^{I_e} \in \mathbb{R}^{p \times z}$ undergo projection to match the dimension of the text representation which results in $\tilde{\mathcal{F}}^{I_e} \in \mathbb{R}^{p \times k}$. The ground truth y is rearranged to get feature-level masks $\tilde{y} \in \mathbb{R}^{p \times w}$ followed by the extraction of positive and negative labels for the feature-level alignment. **Feature-level contrastive alignment loss:** Given the positive label set \mathcal{C}_j^+ and negative label set \mathcal{C}_j^- for each feature-level mask $\tilde{y}_j : j \in [1, p]$, our feature-level contrastive alignment loss \mathcal{L}_{Align} could be represented as

$$\mathcal{L}_{Align} = \mathcal{L}_{pos} + \mathcal{L}_{neg} \quad (2)$$

where we map together the feature level image encoder representation $\tilde{\mathcal{F}}_j^{I_e}$ to the text feature \mathcal{F}_m^T for all the corresponding

positive labels m in the corresponding mask.

$$\mathcal{L}_{pos} = \sum_{j=1}^p \frac{1}{|\mathcal{C}_j^+|} \sum_{m \in \mathcal{C}_j^+} \max \left(0, 1 - \left[\frac{\tilde{\mathcal{F}}_j^{I_e} \cdot \mathcal{F}_m^T}{|\tilde{\mathcal{F}}_j^{I_e}| \cdot |\mathcal{F}_m^T|} \right] \right) \quad (3)$$

Similarly, the possible non-matching label features \mathcal{F}_q^T are pushed away from the visual encoder representations.

$$\mathcal{L}_{neg} = \sum_{j=1}^p \frac{1}{|\mathcal{C}_j^-|} \sum_{q \in \mathcal{C}_j^-} \max \left(0, \left[\frac{\tilde{\mathcal{F}}_j^{I_e} \cdot \mathcal{F}_q^T}{|\tilde{\mathcal{F}}_j^{I_e}| \cdot |\mathcal{F}_q^T|} \right] - 1 \right) \quad (4)$$

By integrating our feature-level contrastive alignment loss, the total loss for supervised training becomes:

$$\mathcal{L} = \mathcal{L}_{Seg} + \mathcal{L}_{Align} \quad (5)$$

4. EXPERIMENTS AND RESULTS

Datasets and Experimental setup: We evaluate our approach in three cross domain settings: 1) cross-modality abdomen, 2) cross-sequence cardiac and 3) cross-site fundus datasets. Dataset details are summarized in Table 1.

Training Details: For cross-modality and cross-sequence experiments, all models are trained on U-Net with Efficient Net-b2 backbone for 2K epochs with inputs size 192×192 and initial learning rate of 3×10^{-4} . For fair comparison with SLAug [5], we follow the same preprocessing steps and dataset split. For cross-site experiments, we used the same training pipeline and preprocessing steps of CCSDG [7] and trained models at 592×592 resolution for 100 epochs with initial learning rate 10^{-2} . We chose BinRushed and Magrabilia as distinct source domains for training and evaluated the model on BASE1, BASE2 and BASE3 target domains. **Evaluation**

Table 3. Quantitative results (Cross-Site Fundus): Our approach outperforms supervised training and CSSDG approach. OC refers to Optic Cup and OD refers to Optic Disc.

Method	BASE1		BASE2		BASE3		Average	
	OD	OC	OD	OC	OD	OC	OD	OC
Supervised	94.71	84.07	94.84	86.32	95.40	87.34	94.98	85.91
BinRushed								
CCSDG [7]	95.73	86.13	95.73	86.82	95.45	86.77	95.64	86.57
CCSDG(Ours)	96.06	86.27	96.03	87.90	95.77	87.07	95.95	87.08
Magrabia								
CCSDG [7]	94.78	84.94	95.16	85.68	95.00	85.98	94.98	85.53
CCSDG(Ours)	95.05	84.55	95.66	88.32	94.92	85.45	95.21	86.10

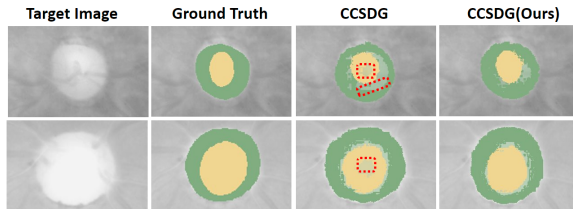


Fig. 2. Qualitative Results (Cross-Site Fundus): CCSDG struggles to accurately define label boundaries (red dashed box), while our approach enhances boundary definition.

Metric: Percentage Dice similarity coefficient [18] is used as the evaluation metric to measure the segmentation performance. **Result Analysis:** Overall, our proposed approach consistently outperforms the baseline methods in all three problem settings. The results of cross-modality Abdomen datasets (Table 2-left) indicates that our approach excels, particularly in the MRI-CT generalization task (2.3% \uparrow) where the performance gap between intra-domain supervised training and SLAug is high. In the cardiac cross-sequence scenario where complexities in resolution are prevalent, our approach manages to enhance the SLAug performance (Table 2-right) despite the small domain gap. For cross-site experiments, incorporating our text-guided contrastive feature alignment approach enhances the model’s comprehension of organ structures and mitigates the impact of background artifacts, leading to improvements in segmentation results across different centers as depicted in Table 3. **Enhanced Organ Boundary Delineation:**

In addition to improvements in the dice score, the qualitative results reveal that our approach enhances the refinement of ROI boundaries and reduces instances of miss classification. This enhancement is crucial for precise organ localization. Visualizations presented in Fig.3 shows that our approach significantly improves the model’s capability to accurately locate and delineate organ boundaries in both CT-MRI and MRI-CT settings. Notably, in the context of cardiac cross-sequence experiments, although the dice score improvement is modest, our approach excels in the precise delineation of organ boundaries, as visually depicted in Fig. 4. Qualitative results from cross-site experiments, as shown in Fig.2, further emphasize that our approach generates accurate segmentation masks by meticulously refining

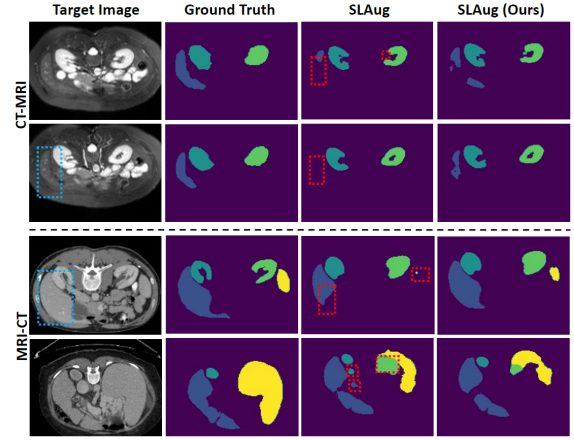


Fig. 3. Qualitative results (Cross-Modality Abdomen): Domain-specific appearance shift :- Liver (blue dashed box) appears dark in MRI (top) and bright in CT (bottom) images. Our approach enhances the SLAug baseline by reducing miss classification (red dashed box) and refining organ boundaries.

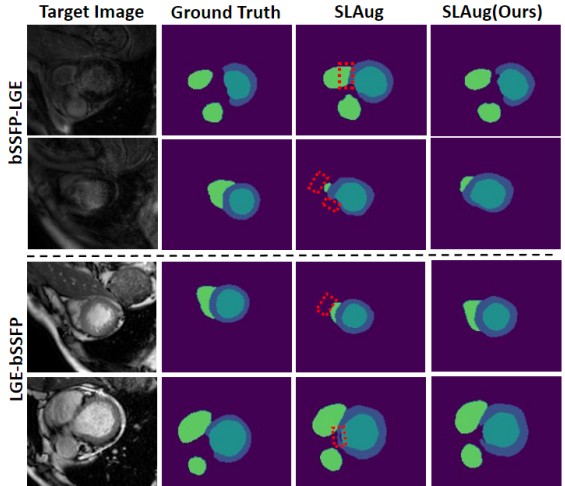


Fig. 4. Qualitative results (Cross-Sequence Cardiac): Our approach outperforms the SLAug baseline in delineating organ boundaries (highlighted by red dashed boxes).

organ boundaries with precision and sharpness.

5. CONCLUSION

This paper introduces an enhancement to single source domain generalization in medical image segmentation by combining textual information with visual features, effectively addressing domain shifts and improving segmentation robustness. The proposed text-guided contrastive feature alignment method demonstrates its efficacy, bringing significant improvements in challenging clinical scenarios, including cross-modality, cross-sequence, and cross-site settings.

6. COMPLIANCE WITH ETHICAL STANDARDS

This study was conducted retrospectively using human subject datasets made available in open access by [13], [14], [15], and [16]. Ethical approval was not required, as confirmed by the licenses attached to the open access data.

7. ACKNOWLEDGMENTS

The authors gratefully acknowledge the scientific support and High Performance Computing (HPC) resources provided by Mohammed bin Zayed University of Artificial Intelligence. No funding was received for conducting this study. The authors have no relevant financial or non-financial interests to disclose.

8. REFERENCES

- [1] Hao Guan and Mingxia Liu, “Domain adaptation for medical image analysis: a survey,” *IEEE Transactions on Biomedical Engineering*, vol. 69, no. 3, pp. 1173–1185, 2021.
- [2] Yaroslav Ganin and Victor Lempitsky, “Unsupervised domain adaptation by backpropagation,” in *International conference on machine learning*. PMLR, 2015, pp. 1180–1189.
- [3] Krikamol Muandet, David Balduzzi, and Bernhard Schölkopf, “Domain generalization via invariant feature representation,” in *International conference on machine learning*. PMLR, 2013, pp. 10–18.
- [4] Cheng Ouyang, Chen Chen, Surui Li, Zeju Li, Chen Qin, Wenjia Bai, and Daniel Rueckert, “Causality-inspired single-source domain generalization for medical image segmentation,” *IEEE Transactions on Medical Imaging*, vol. 42, no. 4, pp. 1095–1106, 2022.
- [5] Zixian Su, Kai Yao, Xi Yang, Kaizhu Huang, Qiufeng Wang, and Jie Sun, “Rethinking data augmentation for single-source domain generalization in medical image segmentation,” in *Proceedings of the AAAI Conference on Artificial Intelligence*, 2023, vol. 37, pp. 2366–2374.
- [6] Ziqi Zhou, Lei Qi, Xin Yang, Dong Ni, and Yinghuan Shi, “Generalizable cross-modality medical image segmentation via style augmentation and dual normalization,” in *Proceedings of the IEEE/CVF Conference on Computer Vision and Pattern Recognition*, 2022, pp. 20856–20865.
- [7] Shishuai Hu, Zehui Liao, and Yong Xia, “Devil is in channels: Contrastive single domain generalization for medical image segmentation,” *arXiv preprint arXiv:2306.05254*, 2023.
- [8] Jean Lahoud, Jiale Cao, Fahad Shahbaz Khan, Hisham Cholakkal, Rao Muhammad Anwer, Salman Khan, and Ming-Hsuan Yang, “3d vision with transformers: A survey,” *arXiv preprint arXiv:2208.04309*, 2022.
- [9] Muhammad Awais, Muzammal Naseer, Salman Khan, Rao Muhammad Anwer, Hisham Cholakkal, Mubarak Shah, Ming-Hsuan Yang, and Fahad Shahbaz Khan, “Foundational models defining a new era in vision: A survey and outlook,” *arXiv preprint arXiv:2307.13721*, 2023.
- [10] Omkar Thawkar, Abdelrahman Shaker, Sahal Shaji Mullappilly, Hisham Cholakkal, Rao Muhammad Anwer, Salman Khan, Jorma Laaksonen, and Fahad Shahbaz Khan, “Xraygpt: Chest radiographs summarization using medical vision-language models,” *arXiv preprint arXiv:2306.07971*, 2023.
- [11] Ling Zhang, Xaosong Wang, Dong Yang, Thomas Sanford, Stephanie Harmon, Baris Turkbey, Bradford J Wood, Holger Roth, Andriy Myronenko, Daguang Xu, et al., “Generalizing deep learning for medical image segmentation to unseen domains via deep stacked transformation,” *IEEE transactions on medical imaging*, vol. 39, no. 7, pp. 2531–2540, 2020.
- [12] Yanwu Xu, Shaoan Xie, Maxwell Reynolds, Matthew Ragoza, Mingming Gong, and Kayhan Batmanghelich, “Adversarial consistency for single domain generalization in medical image segmentation,” in *International Conference on Medical Image Computing and Computer-Assisted Intervention*. Springer, 2022, pp. 671–681.
- [13] Bennett Landman, Zhoubing Xu, J Igelsias, Martin Styner, T Langerak, and Arno Klein, “Miccai multi-atlas labeling beyond the cranial vault–workshop and challenge,” in *Proc. MICCAI Multi-Atlas Labeling Beyond Cranial Vault—Workshop Challenge*, 2015, vol. 5, p. 12.
- [14] A Emre Kavur, N Sinem Gezer, Mustafa Bariş, Sinem Aslan, Pierre-Henri Conze, Vladimir Groza, Duc Duy Pham, Soumick Chatterjee, Philipp Ernst, Savaş Özkan, et al., “Chaos challenge-combined (ct-mr) healthy abdominal organ segmentation,” *Medical Image Analysis*, vol. 69, pp. 101950, 2021.
- [15] Xiahai Zhuang, Jiahang Xu, Xinzhe Luo, Chen Chen, Cheng Ouyang, Daniel Rueckert, Victor M Campello, Karim Lekadir, Sulaiman Vesal, Nishant RaviKumar, et al., “Cardiac segmentation on late gadolinium enhancement mri: a benchmark study from multi-sequence cardiac mr segmentation challenge,” *Medical Image Analysis*, vol. 81, pp. 102528, 2022.

- [16] Shishuai Hu, Zehui Liao, and Yong Xia, “Domain specific convolution and high frequency reconstruction based unsupervised domain adaptation for medical image segmentation,” in *International Conference on Medical Image Computing and Computer-Assisted Intervention*. Springer, 2022.
- [17] Alec Radford, Jong Wook Kim, Chris Hallacy, Aditya Ramesh, Gabriel Goh, Sandhini Agarwal, Girish Sastry, Amanda Askell, Pamela Mishkin, Jack Clark, et al., “Learning transferable visual models from natural language supervision,” in *International conference on machine learning*. PMLR, 2021, pp. 8748–8763.
- [18] Fausto Milletari, Nassir Navab, and Seyed-Ahmad Ahmadi, “V-net: Fully convolutional neural networks for volumetric medical image segmentation,” in *2016 fourth international conference on 3D vision (3DV)*. Ieee, 2016, pp. 565–571.